Journal of Manufacturing Engineering, December 2018, Vol. 13, Issue. 4, pp 216-222

NUMERICAL MODELLING OF LUBRICATED FOIL ROLLING

*** Manoj Kumar, Jyoti Raman and Priya**

[1]Professor & Head, Department of Mechanical Engineering, Echelon Institute of Technology Faridabad, Haryana-121101, India.
[2,3]Maa Yashodhara Private Industrial Training Institute Sambhuganj, District: Banka, Bihar -813211,India.

ABSTRACT

A model of lubricated cold strip rolling (1, 2) is presented to the thin foil regime. The model considers the evolution of asperity geometry and lubricant pressure through the bite, treating the strip using a conventional slab model. The elastic deflections of the rolls are coupled into the problem using an elastic finite element model. A novel modification to these standard friction laws is used to mimic slipping friction in the reduction regions and sticking friction in a central neutral zone. Results are calculated for typical industrial conditions, rolling aluminium foil from a thickness of 50 to 25 μm. In a short inlet region the pressure rises in the lubricant until bulk yielding takes place. Finally it is suggested that in many circumstances it would be appropriate to simplify the model by calculating the details of the tribology only in the short inlet region. This would improve convergence and robustness considerably.

Key words: *Metal rolling, Mixed regime, Roll deformation.*

1. Introduction

Industry is increasingly concerned to develop models of cold rolling, both to improve their on-line control, and to optimise mill set-up and scheduling. Two factors make foil modelling particularly demanding. Firstly, it is essential to model the elastic deformation of the rolls accurately. Secondly, as the ratio of the bite length to the strip thickness increases, the load and reduction in gauge become increasingly sensitive to friction, requiring an accurate mathematical model of friction. The foil rolling model of [1], which has become widely accepted in industry, combines elastic deformation of the rolls and an elastic-plastic model of the foil. They assume that friction between the roll and strip can be modelled using a Coulomb friction coefficient, typically using a value of 0.03. The contact length is split into a series of zones, depending on whether the strip is plastic or elastic and whether there is slip between the roll and strip. At the thinner gauges the solution predicts a central flat, no-slip region, where friction falls below the limiting value for slipping. This model has been extended by [2] and [3]. An alternative strategy which overcomes numerical difficulties associated with the above procedure is described by [4]. They define an arbitrary friction law which simulates sticking friction in the neutral zone and slipping friction elsewhere. This approach is presented by using a physically-based friction law in the neutral zone [5]. An approximation to the lubrication conditions in the contact can be made by estimating the oil film thickness h_s according to [6] formula for smooth rolls and strips:

$$h_s = \frac{6\eta_0 \alpha \bar{u}}{\theta_0 \left(1 - \exp\left(-\alpha Y\right)\right)} \quad \textbf{[1]}$$

where $\bar{u} = \left(u_r + u_{s0}\right)/2$ is the mean of the roll and strip inlet speeds, θ_0 is the inlet angle between the strip and roll and Y is the plain strain yield strength of the strip. η_0 is the viscosity of the lubricant at ambient pressure and α is the Barus pressure viscosity coefficient. The ratio $\Lambda_s = h_s/\sigma_{t0}$ of the smooth film thickness h_s to the combined roll and initial strip roughness σ_{t0} is used to characterise the lubrication regime. In industrial rolling, the needs for high productivity but good surface finish dictate that rolling is commonly in the 'mixed' regime with Λ_s between 0.01 and 0.5. The change in oil pressure is modelled using Reynolds equation, suitably modified to include the effect of roughness. The effect of bulk deformation on the asperity crushing behaviour can be described using the results of [7]. Two approaches have been used to combine the lubrication details with an overall model of the bite. Either an inlet analysis can be used, in which it is assumed that the tribology of the contact is determined in a short inlet region [8]. Alternatively, the

**Corresponding Author - E- mail: kumarm1968@rediffmail.com*

plasticity and tribological details are modelled through the bite [9]. These models calculate the variation of lubricant film thickness through the bite and hence the area of contact ratio *A*, i.e. the fraction of the surface for which the asperity tops are in contact. The remaining valley regions are separated by oil. The friction stress is found by adding contributions from these two areas. Results show that the film thickness and area of contact ratio depend primarily on the rolling speed, oil properties and inlet geometry. The effects of yield stress, strip thickness, asperity geometry and unwind tension are of secondary importance. Experimental measurements of film thickness are in good agreement with theoretical predictions [10]. For foil rolling, it is necessary to model both roll elastic deformation and the tribology. It described such a model, but only considers the case where there is limited roll elasticity [11]. In this paper that model is presented to the thin foil regime where there is a central flat section.

2. Theory

In this paper, we present a model of the thin foil regime where the roll deformations are large, a new friction model is introduced in this paper, as described below, to overcome numerical difficulties.

2.1. Friction Modelling

It is showed that both slipping and sticking between the roll and strip need to be considered in foil rolling. For the regions of slipping, either a Coulomb friction coefficient μ_a or a Tresca friction factor m_a is used to estimate the shear stress τ_a on the asperity tops as

$$\tau_a = \mu_a p_a \qquad [2]$$

wherep_a is the pressure on the asperity tops and *k* is the shear yield stress of the workpiece. To simulate the sticking region, where the shear stress falls below the value for slipping friction (equation 2), the approach is followed in adopting an arbitrary friction law. A knockdown factor δ on the limiting friction is applied to [2], so that $\tau_a = \delta\mu_a p_a$, with

$$\delta = \frac{\theta}{\sqrt{\theta^2 + (\varepsilon\theta_1)^2}} \qquad [3]$$

whereε is a tolerance parameter, θ is the local roll slope and θ_1 is a representative roll slope in a slipping region (see Fig. 3). Here θ_1 is taken as the slope at the middle of the first reduction region. This variation of δ with θ/θ_1 is sketched in Fig. 1. For $\theta/\theta_1 \ll \varepsilon$ the frictional stress is approximately proportional to the roll slope while, for $\theta/\theta_1 \gg \varepsilon$,$\delta$ approaches one and friction takes its limiting value of $\mu_a p_a$ .Changes in friction in the central sticking region can be accommodated by small deviations in flatness. As long as ε is sufficiently small, the roll stays essentially flat there and the solution is unaffected by the exact form of the friction law. Typically a value of ε = 0.1 was found appropriate. A physically-based argument for a friction law of this form is presented [12].The shear stress in the valleys τ_b is estimated from the Newtonian viscous behaviour of the oil, with a constant valley depth of$h_t/(1-A)$, where h_t is the mean film thickness.

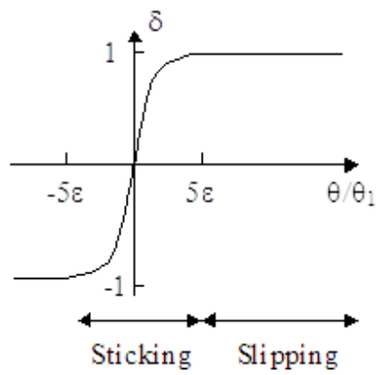

Figure 1. Schematic variation in knockdown factor δ with roll slope θ used to simulate sticking and slipping friction.

The lesser of this hydrodynamic estimate and the corresponding shear stress τ_a on the asperity tops is used for the valley regions. The average shear stress τ is given by a weighted sum of the asperity and valley contributions

$$\tau = A\tau_a + (1-A)\tau_b \qquad [4]$$

2.2. Strip deformation

A standard slab model is used for the strip. Equilibrium for a slab in the bite gives

$$t\frac{d\sigma_x}{dx} + (\sigma_x + p)\frac{dt}{dx} + 2\tau = 0 \qquad [5]$$

Where x is the distance in the rolling direction, t is the strip thickness, □ x is the tensile stress in the rolling direction and p is the average contact pressure. In the inlet and exit regions, where there is no plastic

deformation, it is assumed that the strip is linear-elastic. In the central reduction region the strip is taken as perfectly plastic, and at the point of yield, so that

$$\sigma_x + p = Y \qquad [6]$$

2.3. Roll elasticity

A standard elastic FEM package is used to solve the roll deformation equations for a given pressure distribution.

2.4. Hydrodynamic modelling

The variation in oil pressure p_b through the bite is given by Reynolds equation, modified to include the effect of roughness:

$$\phi_x \frac{h_t}{12\eta}\frac{dp_b}{dx} = \frac{u_x + u_r}{2}h_t + \frac{u_x - u_r}{2}\sigma_t\phi_s - Q \qquad [7]$$

Where u_x is the local strip velocity and Q is a flow rate constant. Flow factors ϕ_x and ϕ_s, which are functions of the mean film thickness h_t and the combined strip and roll roughness σ_t, are derived. They also depend on γ, the ratio of roughness correlation lengths in the rolling and transverse direction. Here γ is taken equal to 9, appropriate for nearly longitudinal roughness. As the oil film becomes smaller, it is shown that a 'percolation threshold' is eventually reached when individual pockets of oil become trapped. This occurs, for longitudinal roughness with $\gamma = 9$, when $h_t/\sigma_t = 0.038$. For the results presented here the film thicknesses are significantly greater than this percolation threshold. Where the film thickness approaches the percolation threshold, micro-plasto-hydrodynamic models are needed.

2.5. Asperity Flattening

To derive an accurate estimate of the change in asperity geometry and contact area through the bite, is essential to include the effect of bulk plasticity on changes in asperity deformation. In this paper, the model for crushing of longitudinal roughness is presented. This uses a curve fit to the finite element calculations.

2.6. Numerical Method

The details of the numerical method are described here. In this paper, a double-shooting procedure is used to find the inlet strip speed and oil flow rate constant Q for a given roll shape. The differential equations for the variation of pressure and contact ratio through the bite are integrated using a Runge-Kutta method. Once a converged pressure distribution is found, the corresponding strip shape t_C is solved using the FE model for the roll elastic deformations. The new roll shapet_{N+1} is related to the old roll shape t_N and the computed roll shape t_C, based on the current pressure distribution, by the relaxation formula

$$t_{N+1} = \beta t_C + (1-\beta)t_N \qquad [8]$$

Typically a relaxation coefficient βbetween 0.2 and 0.05 is suitable, giving computation times of the order of 2 hours on a small super-computer for the most demanding cases.

3. Results

In this section, we present results typical of industrial rolling of aluminium foil from a thickness of 50 µm to 25 µm, lubricated with standard rolling oil. Conditions are detailed in Table 1.

Table 1: Summary of conditions

Strip	Entry Gauge	50 µm
	Exit Gauge	25 µm
	Yield Stress	150 MPa
	Unwind Tension	20 MPa
	Rewind Tension	20 MPa
	Young's Modulus	70 GPa
	Poisson's Ratio	0.3
Rolls	Radius	135 mm
	Roll Peripheral Speed	5–40 m/s
	Young's Modulus	210 GPa
	Poisson's Ratio	0.3
Surfaces	Combined r.m.s. amplitude	0.3 µm
	Asperity wavelength	30 µm
	Asperity friction	$\mu_a = 0.1$
Lubricant	Viscosity at ambient pressure	2.5×10^{-3}Pas
	Pressure viscosity coefficient	$1.2\times10^{-8}m^2/N$

Fig. 2 shows the distribution of average pressure p, average shear stress τ and area of contact ratio A for a rolling speed of 20 m/s with a Coulomb friction factor $\mu_a = 0.1$.

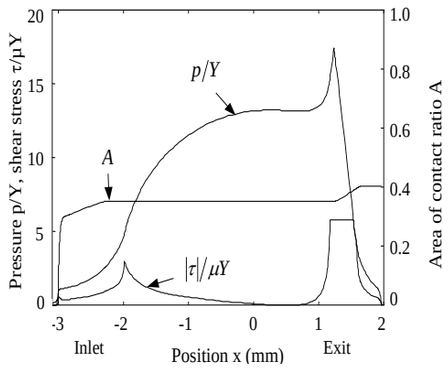

Figure 2: Variation in pressure, shear stress and area of contact ratio through the bite;ur= 20 m/s, μa = 0.1

The normal pressure is normalised by the yield stress Y and the shear stress by $\mu_a Y$, so that the shear curve lies on the pressure curve when the effective contact area A and the friction knockdown factor δ are both equal to one.

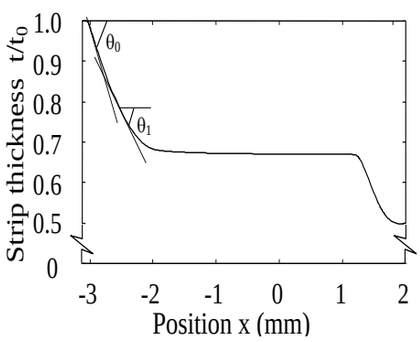

Figure 3: Variation in strip thickness through the bite, u_r = 20 m/s, μ_a = 0.1

Angle θ is the local slope of the roll profile, θ_0 its value at bite entry, θ_1 at the centre of the first deformation zone.

Fig. 3 shows the corresponding change in strip thickness t through the bite, normalised by the inlet strip thickness t_0. These results have a similar form to those of [13], with a significant 'flat' sticking region at the centre of the bite where the shear stress falls below its limiting value. Fig. 2 shows that, for the Coulomb friction model, the frictional stress equals the shear yield stress of the strip over a significant portion of the exit reduction region (where the shear stress has a plateau). Because of the high pressures directly after this region of the bite, the estimated hydrodynamic shear stress would exceed the asperity shear stress. Hence the average shear stress is taken equal to $\mu_a p$, the effective contact area equals one and the curves for shear and normal pressure lie on top of one another.

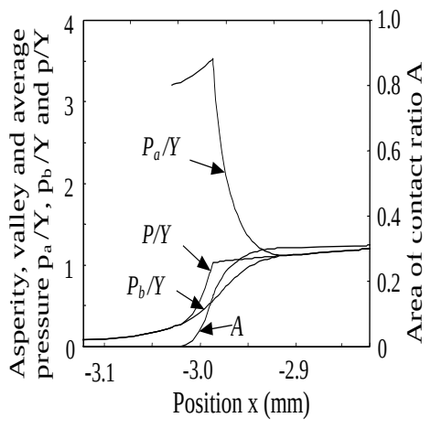

Figure 4: Variation of asperity, valley and average pressure and area of contact ratio in the inlet; u_r= 20 m/s, μ_a = 0.1

Details at the inlet are illustrated in Fig. 4, showing the change in normal pressure p, asperity and hydrodynamic pressures p_a and p_b and area of contact ratio A. Comparing the scales on Fig. 2 and 4 it is clear that the inlet region is very short compared with the length of the bite. At the beginning of the inlet, before the hydrodynamic pressure has built up, the asperity pressure is approximately equal to the hardness $3Y$. As the pressure in the lubricant build ups, the strip yields, causing a sharp change in the slope of the mean pressure curve and a drop in the asperity pressure. At this point the asperity tops are rapidly flattened and the valley pressure rapidly rises to equal the asperity pressure. Through the remainder of the bite, the model assumes that the valley pressure $p_b$remains equal to the asperity pressure p_a. The area of contact ratio A increases slightly through the rest of the bite due to thinning of the oil film as the strip surface elongates, Fig. 2.

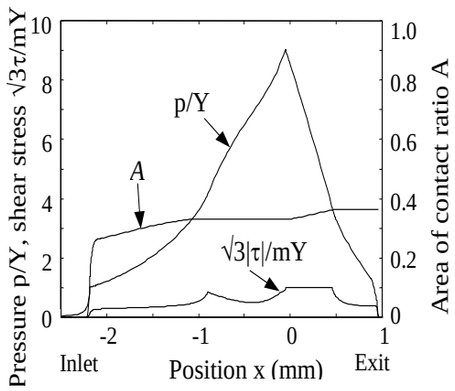

Figure 5. Variation in pressure, shear stress, and areaof contact ratiothe bite; u_r = 20 m/s, m_a= 0.25

Fig. 5 shows the variation through the bite of the normal pressure p, the shear stress τ and area of contact ratio A, for the same conditions as Fig. 2, but with a friction factor $m_a = 0.25$ instead of a friction coefficient $\mu_a = 0.1$. These values of friction factor and friction coefficient have been chosen for comparison to give approximately the same mean frictional stress and rolling loads at high rolling speeds where there is only a slight friction hill. (In fact the two laws give the same stress for $p = 1.4Y$.) The friction factor approach gives lower shear stresses in the high pressure regions where $p > 1.4Y$, and so a significantly lower average pressure. The frictional stresses are normalised by $m_aY/\sqrt{3}$, so that this expression equals one when the effective contact area and the friction knockdown factor δ are both equal to one.

3.1. Effect of speed

Fig. 6 shows the effect of rolling speed on roll load, using a logarithmic axis for load. The change in speed from 5 to 40 m/s corresponds to a range of film thickness parameter Λ_s from 0.22 to 1.76. Although the smooth film thickness, equation 1, is based on the slope of the undeformed roll at the inlet, in fact the slope of the deformed roll is not very different for the cases presented here. Hence this smooth film thickness is representative.

The graph includes the cases of a friction coefficient of 0.1 and a Tresca friction factor of 0.25. Corresponding changes in the forward slip and the mean film thickness h_t/σ_{t0} and area of contact ratio A at the exit are plotted in Fig. 7. As the speed falls, there is a reduction in the thickness of the oil film drawn through the contact h_t/σ_{t0} and the area of contact ratio rises accordingly. The associated increase in frictional stress causes a large increase in rolling load, as observed experimentally. A flat region in the bite is predicted below speeds of about 20 and 30 m/s for the friction coefficient and friction factor approaches, respectively. The marked difference in load between the Tresca and Coulomb friction models, Fig. 6, reflects the sensitivity of results to the details of the friction distribution, despite the relatively slight changes in the film thickness and area of contact estimates (Fig. 7).

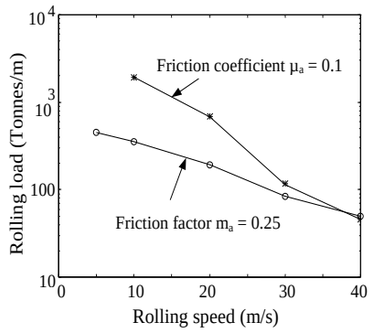

Figure 6: Effect of rolling speed on roll load

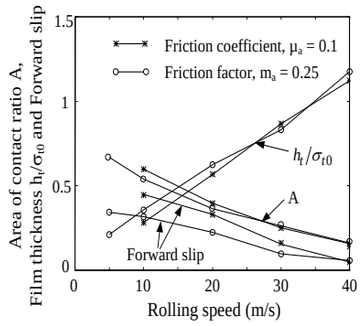

Figure 7: Effect of rolling speed on area of contact ratio, film thickness and forward slip

4. Discussions

Figures 6 and 7 confirm that the key rolling parameters – load and forward slip – are sensitive to the details of the frictional model. An appropriate choice of friction model must rely either on a comparison with experimental measurements or some physical insight

into the interface behaviour in the bite. Both approaches are currently being explored. As Figure 4 shows, the inlet region is very short compared with the bite region for the conditions considered here. This could be expected with mixed lubrication and typical roll roughness's and strip reductions. These have constructed a regime map for thick strip rolling which shows that this is true for most practical purposes. In this paper with foil rolling, the small value of t/λ, the ratio of the strip thickness to the roughness wavelength, increases the ease with which asperities can be crushed. Hence the inlet will be small compared with the bite over an even wider range of operating conditions. This observation suggests that it would be appropriate in most cases to consider all the tribological details only in the inlet. A much-simplified model of the contact could be used to estimate the change in friction through the bite. With this approach there is limited coupling between roll deformation and lubrication, which would give a much simpler and more robust analysis. The characteristic roughness wavelength λ was taken in this analysis as 30μm. In this paper it is investigated the effect of roughness wavelength, considering more than one wavelength. The results and subsequent work in progress suggest this single value characterises the spectrum of roughness reasonably well for typical aluminium foil rolling conditions.

5. Conclusions

A tribological model of cold strip rolling [1, 2] is presented to the thin foil rolling where the elastic deflections of the rolls become significant. This model calculates the variation of asperity geometry and lubricant pressure through the bite and uses a conventional slab model of the strip. An elastic finite element model is used to calculate roll deflections. A previous model of foil rolling [3] predicts reduction zones at the entry and exit to the bite, with a flat neutral zone where there is limited relative slip between the roll and strip. This observation is used to construct an arbitrary modification to the standard friction laws which simulates this behaviour, with friction proportional to the roll slope in the sticking region and equal to the limiting friction value in the slipping regions. Either Coulomb and Tresca friction models are used in the slipping regions for contact between the rolls and asperity tops, while the frictional stress in the valleys is estimated from the viscous shearing of the oil. In the case of Coulomb friction, the frictional stress is limited to the shear yield stress of the strip.

Results are calculated for typical industrial conditions, rolling aluminium foil from a thickness of 50 to 25 μm. In a short inlet region the pressure rises in the lubricant until bulk yielding takes place. At that point the asperities are rapidly crushed until the lubricant and asperity pressures equalise. The effect of a variation in rolling speed from 5 to 40 m/s on rolling load, film thickness and cross sectional area is examined. As the speed falls, the forward slip is predicted to increase from a value of 5 to 45% for the Coulomb friction model. The increase in forward slip is much less marked for the Tresca friction model. Finally it is suggested that in many circumstances it would be appropriate to simplify the model by calculating the details of the tribology only in the short inlet region. This would improve convergence and robustness considerably.

Acknowledgement

The authors express their sincere thanks to MaaYashodhara Industrial Training Institute, Sambhuganj, Banka, Bihar, India and colleagues of that stream. The corresponding author expresses his earnest thanks to the co-authorsMiss Jyoti Raman and Miss Priya, MaaYashodhara Industrial Training Institute, Sambhuganj, Banka, Bihar, India. The author also acknowledges to reviewers of JME for their careful reading of our manuscript.

References

1. *Joze Valemtincic, Kusen D, Smrkolj S, Oki Blatnink and Mihael Junkar (2007), "Machining parameters selection for varying surface in EDM", Int. J. Materials and product Technology, Vol. 29, 1/2/3/4.PageNo.*

2. *Rozenek M, Kozak J, Dabrswski L and Lubkowski K (2001), "EDM Characteristics of MMCs", Journal of Materials Processing Technology, Vol. 109, 367-370.*

3. *Koenraad Bonny, Patric de Baets, Jozef Vleugels, Salehi A, Omer Van derBiest, Bert Lauwers and Wenqing Liu, (2008), "EDM machinability and frictional behaviour of ZrO2-WC composites", International Journal of Advanced Manufacturing Technology, Vol. 41(11), 1085-1093.*

4. *Su J C, Kao J Y and Tarng Y S (2004), "Optimization of the electrical discharge machining process using a GA-based neural network", International Journal of Advanced Manufacturing Technology, Vol.24, 81-90.*

5. *Shajan kariahose and Shunmugam M S (2005), "Multi-objective optimization of WEDM process by GA", Journal of Materials Processing Technology, Vol. 170, 133-141.*

6. *Mu-Tian yan and Chi-Cheng Fang (2008), "Application of genetic algorithm-based fuzzy logic control in EDM machine", Journal of Material Processing Technology, Vol. 205, 128-137.*

7. *Asthana R (1998), "Processing effect on the properties of cast of metal matrix composites" University of Wisconsil-Stout, Menomonie WI 54751, Vol No., 213-255.*

8. *Lindroos V K and Talvitie M J (1995), "Recent advances in metal matrix composites" Journal of Material Processing Technology, Vol. 53, 273-284.*

9. *Bhaskar reddy C, Diwakar reddy V and Eswara reddy C (2012), "Experimental Investigations On Mrr And Surface Roughness Of EN 19 & SS 420 Steels In Wire Edm Using Taguchi Method" International Journal Of Engineering Science And Technology, Vol. 4 (11), 4603-4614.*

10. *Harsimran Singh and Harmesh Kumar (2015), "Review On Wire Electrical Discharge Machining (WEDM) Of Aluminum Matrix Composites" International Journal of Mechanical and Production Engineering, Vol.3 (10) 1-5.*

11. *Nataraj M and Ramesh P (2016), "Investigation on Machining Characteristics of Al 6061 Hybrid Metal Matrix Composite Using Electrical Discharge Machining", Middle-East Journal of Scientific Research, Vol.24 (6), 1932-1940.*

12. *Fleck, A., Johnson, L., Mear, E., and Zhang, C. (2012), "Cold rolling of foil".Proc. Instn. Mech. Engrs, Vol.206, 119-131.*

13. *Dixon, E., Yuen, D. (1995), "A computationally fast method to model thin strip rolling", Proc. Computational Techniques and Application Conference, Vol 37, 239-246.*

14. *Domanti, A, Edwards, J, Thomas, J, and Chefneux L (2014), "Application of foil rolling models to thin steel strip and temper rolling" Proc. 6th International Rolling Conference, Vol 4, 422-429.*

15. *Gratacos, P, Montmitonnet, P, Fromholz, C, and Chenot L (2012), "A plane-strain elastic finite-element model for cold rolling of thin strip", International Journal of Mechanical Sciences, Vol. 34(3), 195-210.*

16. *Le R, and Sutcliffe, F (2009), "A robust model for rolling of thin strip and foil", Int. J. of Mechanical Sciences, Vol. 3, 132-151.*

17. *Wilson D and Walowit A (1972), "An Isothermal Hydrodynamic Lubrication Theory for Strip Rolling With Front and Back Tension". Proc. 1971 Tribology Convention, I. Mech. E., London, Vol No, 164-172.*

18. *Sutcliffe F and Johnson L (2017), "Lubrication in cold strip rolling in the 'mixed' regime", Proc. Instn. Mech. Engrs., Vol. 204, 249-261.*

19. *Wilson D and Sheu S (2008), "Real Area of Contact and Boundary Friction in Metal Forming". Int. J. Mech. Sci., Vol. 30, 475-489.*

20. *Marsault N, Montmitonnet P, Deneuville P and Gratacos P (2016), "A Model of Mixed Lubrication for Cold Rolling of Strip", Proc.NUMIFORM 16, Twente University, Netherlands, A.A. Balkema (Rotterdam), Vol 6, 715-720.*

21. *Wilison, W., and Maarsault, N. (2008), "Partial hydrodynamic lubrication with large fractional contact areas" ASME, J. Tribology, Vol.120, 1-5.*

22. *Patir N and Cheng S (1978), "An average flow model for determining effects of three dimensional roughness on partial hydrodynamic lubrication", ASME J. Lubrication Technology, Vol. 100, 12-17.*

23. *Lo S (1994), "A Study on the Flow Phenomena in the Mixed Lubrication Regime by Porous Medium Model", ASME J. Tribology , Vol.116, 640-647.*

24. *Sheu S and Wilson D (2014), "Mixed lubrication of strip rolling", STLE Trib. Trans., Vol.3, 483-493.*

Nomenclature

A	Area of contact, mm^2
h_t	Mean film thickness. mm
h_s	Smooth film thickness, mm
K	Shear yield stress, MPa
m_a , m_b	Friction factor
p	Mean contact pressure, m^2/N
p_a , p_b	Pressure on the asperity tops, N/m^2
R	Roll radius, mm
t, t_0	Strip thickness, inlet thickness, mm
$\overline{u}$	Mean entraining velocity, m/s
u_r, $u_s(u_{s0})$	Roll and strip speed, m/s
X	Co-ordinate in rolling direction, mm
Y	Plane strain yield stress of the strip, MPa
α	Oil pressure viscosity index, Pas
δ	Knock-down factor
ε	Tolerance for strip slope
$\eta(\eta_0)$	Viscosity of lubricant, Pas
λ	Wavelength of the surface roughness, mm
μ_a , μ_b	Coulomb coefficient of friction
Λ_s	Speed parameter, m/s
θ, θ_a, θ_l	Roll slope
σ_1, (σ_{rd})	Combined r.m.s. surface roughness, m/s
σ_x	Longitudinal tension stress, MPa
τ	Mean shear stress between roll and strip, MPa